이학석사 학위논문

Synaptic scaffolding protein, nArgBP2, plays a role in dendritic spine formation by controlling actin cytoskeleton

액틴 세포골격 조절을 통한 시냅스 구조 단백질(nArgBP2)의 수상돌기 가시 형성에서의 역할

2013년 2월

서울대학교 대학원

뇌과학 협동과정

한정규

Synaptic scaffolding protein, nArgBP2, plays a role in dendritic spine formation by controlling actin cytoskeleton

지도교수 장 성 호

이 논문을 한정규 석사학위논문으로 제출함

2012 년 11 월

서울대학교 대학원

뇌과학 협동과정

한정규

한정규의 석사학위논문을 인준함

2012 년 11 월

위 원 장 박 동 은 (인)

부 위 원 장 장 성 호 (인)

위 원 최 석 우 (인)

Synaptic scaffolding protein, nArgBP2, plays a role in dendritic spine formation by controlling actin cytoskeleton

By

Jeong-Kyu Han

A Thesis Submitted to the Department of Natural Science in Partial Fulfillment of the Requirements for the Degree of Master in Interdisciplinary Program in Neuroscience at Seoul National University

February 2013

Approved by thesis committee:

Professor	_____	**Chairman**
Professor	_____	**Vice Chairman**
Professor	_____	**Member**

Abstract

Synaptic scaffolding protein, nArgBP2, plays a role in dendritic spine formation by controlling actin cytoskeleton

Jeong-Kyu Han

Interdisciplinary Program in Neuroscience

The Graduate School

Seoul National University

Dendritic spines are small actin-rich protrusions that function to receive the excitatory synaptic transmission, which is crucially related to the synaptic plasticity. Hundreds of proteins take part in synaptic activity, consisting of networks in a small dendritic spine with spine head volumes ranging 0.01 μm^3 to 0.8 μm^3. Representatively, WAVE regulatory complex is well-known as mediating upstream signal Rac1 to the activation of the Arp2/3 complex, arranging actin cytoskeleton. In relation to SH3 interactor, WAVE cooperates with nArgBP2 and other adaptor proteins. However, our understanding of nArgBP2 is limited, and properties of nArgBP2 are merely inferred from non-neuronal cell biology. nArgBP2 is a neuronal specific splice variant of ArgBP2 and an adaptor protein of Ponsin/ArgBP2/Vinexin family, and is

enriched postsynaptically. nArgBP2 has a sorbin homology (SoHo) domain in the N-terminal region, a zinc finger in the middle, and three src homology (SH) 3 domains in the C-terminal region. Via its SH3 domains, nArgBP2 interacts with SAPAP, dynamin, synaptojanin, and WAVE isoforms. RNA interference-mediated knock-down of nArgBP2 has a strong effect in dendritic spines of developmental hippocampal neurons. In the developing stage, nArgBP2 knock-down shows a distinct reduction in the number of dendritic spines, but enhances the number of filopodia. Rescue experiments show that knock-down effects are recovered in terms of the number of dendritic spines in the developing stage. When knocking down nArgBP2 in the mature stage, there are no changes in the number of dendritic spines. From live cell imaging, knocking down of nArgBP2 alters shapes and motility of dendritic spines in the developing stage. FRAP (fluorescence recovery after photobleaching) experiments prove that the mobile fraction of actin is increased in the depletion of nArgBP2. In conclusion, nArgBP2 plays a role in dendritic spine formation in the developing stage, organizing synaptic architecture through actin cytoskeleton.

Keywords: dendritic spines, filopodia, RNA interference, actin dynamics, WAVE (WASP-family verprolin homology protein), synaptic morphogenesis

Student Number: 2010-20399

CONTENTS

LIST OF FIGURES

I. Introduction

Dendritic spines are small actin-rich protrusions that contact with the presynaptic membranes and function to receive the excitatory synaptic transmission, which mediated the synaptic plasticity (1). Spines have vigorous changes in morphology during neural development, and adopt a variety of architecture, which can be categorized by several types, such as mushroom, thin, cupped, and stubby (2). In the developing stage, dendritic spine formation ardently occurs, and at the same time filopodia are highly sufficient and have rapid extension and retraction within minutes to hours (3). In order to understand how mechanisms of spine formation and elimination are regulated, intrinsic genetic programs in dendritic spines should be considered.

Actin regulation in dendritic spines plays a pivotal role in spine morphology. In migrating cells, actin polymerization is likely to create protrusions with two-mode: a linear mode and a branched mode. The thin, linear mode of dendritic protrusions is propelled by formins (e.g. mDia1, 2 and 3), while a branched mode of dendritic precursors is nucleated by the Arp2/3 complex, which attaches to the side of an actin filament and promotes growth of another actin filament at a 70° angle (4). Cortactin, N-WASP, WAVE-1, and Abp1 are regulating Arp2/3 complex, following actin-signaling pathway (5). Src family kinases initiate activation of cortactin (6). Cdc42, Rac and PIP_2 trigger N-WASP (7). Rac and PIP_3 binding activate WAVE-1 (8). However, the actin cytoskeleton regulation and its dynamics are still

unanswered with a series of synaptic adaptor proteins.

Among numerous actin-bound proteins regulating actin directly or indirectly, WAVE regulatory complex is well known as mediating upstream signals to the activation of the Arp2/3 complex, guiding to a burst of actin polymerization (9). WAVE regulatory complex is settled as a pentameric heterocomplex that consists of WAVE, ABI, NAP1 (also known as p125NAP1), SRA1 (or the closely related PIR121; SRA1 is also known as CYFIP1**)** and HSPC300 (also known as BRICK) (10) (11) (12). When the upstream signal of Rac1, small GTPase, activates WAVE regulatory complex, through linking of IRSp53, SRA1 and NAP1 are dissociated from WAVE regulatory complex (13) because the VCA region of WAVEs is inhibited before by intracomplex interaction, probably between the VCA region and the SRA1-NAP1 subcomplex (14) (15). The VCA region, especially verprolin-homology domain, recruits and binds a monomeric actin to activate the Arp2/3 complex toward actin polymerization (16).

In addition, isoforms of WAVE are localized in different tissue distribution. WAVE1 and WAVE3 are abundant in the brain, although they are localized over the mammalian body. Moreover, WAVE2 is expressed ubiquitously (17). In relation to SH3 domain interactor, WAVE1 cooperates with WRP, Vinexinβ, and p47phox, and WAVE2 interacts with IRSp53, nArgBP2, and Vinexinβ (9). First of all, WRP combined to WAVE-1 plays a role in the cytoskeletal controls managing neuronal development and synaptic plasticity normally (8). Gain and loss of function study of IRSp53 revealed that PSD-95 interaction is an important determinant factor in synaptic IRSp53

localization and that the SH3 domain of IRSp53 attaches to activated Rac1/Cdc42 to affect downstream signaling for the regulation of dendritic spine morphogenesis (18). Lastly, vinexin β modulates the proteasome-dependent degradation of WAVE2 in a PKA-dependent manner (19). Although most of adaptor proteins associated with WAVE complex are explained regarding a synaptic property, the function of nArgBP2 is limited to understand merely by inferring from non-neuronal cell biology.

As a postsynaptically enriched adaptor protein, nArgBP2 (neural Abelson-related gene binding protein 2) was originally identified as a neural specific splice variant of ArgBP2 (20). The mRNA level of nArgBP2 indicates that it is notably expressed in cortex, striatum, and amygdala, which are the brain regions associated with bipolar disorder, (US Patents. Pub. No.:US 20100077493 A1) (21). As a member of Ponsin/ArgBP2/Vinexin family, nArgBP2 has a sorbin homology (SoHo) domain in N-terminal region, a zinc finger motif in the middle, and three src homology (SH) 3 domains in the C-terminal region. In particular, a zinc finger motif is inserted in neuron-specific nArgBP2 (20). Thanks to this domain composition, nArgBP2 is also named as sorbin and SH3 domain containing 2. Via its SH3 domains, nArgBP2 interacts with SAPAP, dynamin, synaptojanin, and WAVE isoforms. These binding partners commonly contain proline-rich domain. Along with SoHo domain, nArgBP2 interacts with α2-spectrin (22). This protein is thought to play a role in the assembling of signaling complexes, being a connection between Abl kinase and actin cytoskeleton.

In this study, we target genetic control of synaptic morphogenesis to

one of the postsynaptic enriched proteins, nArgBP2, which is thought to be closely related to psychiatric disorders such as bipolar disorder. Those results will shed lights on revealing the function of nArgBP2 at the synapses.

II. Materials and Methods

Ethics statement

All experiments using animals were performed in agreement with guidelines set forth by the Seoul National University Council Directive for the proper care and use of laboratory animals.

DNA constructs and antibodies

Full-length HA-tagged rat nArgBP2 cDNA (amino acids 1-1196) was gently conferred by G. Cestra from University of Rome, La Sapienza. GFP-tagged nArgBP2 was manipulated by subcloning the full-length sequence in pEGFP-C1 by PCR. GFP-actin was kindly provided by Gilbert Di Paolo (Columbia University, New York, NY). YFP-PM(plasma membrane) was also generously from De Camilli Laboratory (Yale University, New Haven, CT). Rabbit polyclonal anti-nArgBP2 antibody was originally raised from De Camilli Laboratory and rabbit polyclonal anti-GFP antibody was produced by our lab. Mouse polyclonal anti-β-tubulin was purchased from Abcam. Secondary antibody was HRP-conjugated anti-rabbit from Jackson ImmunoResearch.

RNA-mediated interference and rescue experiments

RNA interference (RNAi)-mediated nArgBP2 knock-down was carried out by chemically synthesized small hairpin RNA (shRNA) duplexes through pU6 expression vector. The targeted sequences of rat nArgBP2 from its cDNA sequence (Gene bank accession number NM_O35413) were 5'-GAAGGACTGGTACAAGACAAT -3' (shRNA#1, nucleotides 582-602 on SoHo domain) and 5'- GTGTCTGACCACAGCGATA -3' (shRNA#2, nucleotides 2095-2113). These sequences are common to rat nArgBP2 cDNA sequence; in particular target sequence of shRNA#1 is present in all eight isoforms of human nArgBP2. The efficiency of shRNAs was examined in GFP-nArgBP2 expressed HEK293T cells. To confirm the artificial effect of the expression vector, the forward primer sequence of scrambled shRNA for #1 was designed; 5' – GAACGACCCGTATGTGACT -3'. (http://www.sirnawizard.com/) The characters indicate the mixed-up target sequence. For RNAi-refractory, silent mutations within shRNA#1 (C588T and C594T) and shRNA#2 (T2100G, C2103T, A2107T, and G2108C) targeting sequence in GFP-nArgBP2 were generated using QuickChange® Site-Directed Mutagenesis Kit (Stratagene, Austin, Texas). All constructs were verified by sequencing. After transfection, cells were cultured for over 72 hr.

Cell culture and transfection

HEK293T cells (ATCC, Manassas, VA) were cultured at 37 °C and 5% CO_2 in Dulbecco's modified Eagle's medium (Invitrogen) supplemented with 10% fetal bovine serum (HyClone, Logan, UT). Transfection was carried out using

Lipofectamine 2000 (Invitrogen), and cells were observed after 36–48 hr. Primary rat hippocampal neurons were prepared as described. (23) Hippocampal neurons were dissected from E-18 Sprague Dawley rat embryos, dissociated with papain (Worthington Biochemical Corp., Lakewood, NJ, USA) and triturated with a polished half-bore Pasteur pipette. The cells (2.5×10^5) in minimum Eagle's medium supplemented with 0.6% glucose, 1mM pyruvate, 2mM L-glutamine, 10% fetal bovine serum, and antibiotics were plated on poly-D-lysine-coated glass coverslips in a 60-mm Petri dish. Three hours after plating, the medium was replaced with basal media Eagle's (Invitrogen) supplemented with 2% B-27, 10 mM HEPES, and 0.5 mM pyruvate or Neurobasal medium (Invitrogen) supplemented with 2% B-27, 0.5mM L-glutamine. 4μM 1-β-D-cytosine-arabinofuranoside (Ara-C, Sigma) was added as needed. Neurons were transfected using the calcium phosphate method and with AMAXA Nucleofector device (Lonza, Basel, Swizterland).

Quantitative analysis and Image acquisition

Filopodia were defined as thin protrusions without a distinguishable head, and spines were defined as protrusions with a length around 4μm. The numbers of dendritic spines and filopodia were counted manually to estimate the density (number per 100μm length of the primary or secondary dendritic branches). Statistical significance was analyzed using two-sample t-test (two-tail) where $p<0.05$ was set as the minimum value of significance. The numbers of dendritic spines were described as mean ± SE (at least three-independent

experiments). Cultured neurons were fixed in 4% paraformaldehyde, 4% sucrose, PBS for 15 min, mounted on a Zeiss fluorescence microscope using a 40x oil-immersion lens (1.25 NA) and a EMCCD camera (iXon887, Andor Technologies, Belfast, Northern Ireland) by MetaMorph Imaging software (Universal Imaging Corporation, West Chester, PA).

Live cell imaging and FRAP (fluorescence recovery after photobleaching) analysis

For live cell imaging, the culture medium was replaced with pre-warmed Tyrode's solution (119mM NaCl, 2.5mM KCl, 2mM $CaCl_2$, 2mM $MgCl_2$, 25mM HEPES, pH 7.4 and 30mM glucose). The images were obtained using a 63x oil-immersion lens (1.3 NA) equipped with a Zeiss fluorescence microscope. Time-lapse images of hippocampal neurons in 15 to 16 days *in vitro* were recorded at 5 sec of intervals for 5 min. FRAP experiments were performed using a stimulus setting menu in A1 software to control sequential image acquisition using a 60x oil-immersion lens (1.49 NA) equipped with a A1R confocal microscope (Nikon) and emission of a photobleaching laser pulse to the circular ROI (region of interest). A single dendritic spine of hippocampal neurons was set as ROI and two pre-photobleaching images acquired with 5 sec of intervals, and the fluorescence of spine photobleached for 7 sec with an Argon 488 laser. The recovery of fluorescence was traced for 5 min by acquiring images at 5 sec of intervals. In this FRAP experiment, an individual dendritic spine was rapidly photobleached using high-intensity

laser illumination. Pre-bleaching, bleaching and post-bleaching images were utilized for analyzing the actin dynamics. The average intensity values of ROI, and total image fluorescence were obtained from FRAP images. Subsequently, the recovery curve was plotted with the ROI value over the time-dependent manner. Based on the plot, mobile and immobile fractions were calculated to measure the kinetics of GFP-actin. Mobile and immobile fractions were determined by calculating the ratios of the final to initial fluorescence intensity. Fluorescence intensities of the end time-point (F_{end}), start time-point (F_{pre}) and time-point after photobleaching (F_{post}) were formulated as following equations and mobile/immobile fraction was calculated (24) :

$$\text{Mobile fraction} = \frac{(F_{end} - F_{post})}{(F_{pre} - F_{post})}$$

Immobile fraction = 1- Mobile fraction

Western blot

HEK293T cells were transfected with GFP-nArgBP2, shRNA#1, 2, scrambled shRNA#1, 2, and shRNA-resistant, and the cells were washed three times with cold PBS. Immunoblotting was performed from cell lysates generated in RIPA buffer (20 mM Tris, pH 7.5, 100 mM NaCl, 50mM NaF, 1% Nonidet P-40, 0.1% DOC, 1.0% SDS, 1mM orthovanadate) in the presence of a protease inhibitor cocktail (Roche). Protein concentrations in soluble fraction were measured using a Bicinchoninic acid (BCA) Protein Assay Reagent kit (Pierce). The extracted proteins were analyzed by SDS-PAGE (8% gel), and

transferred to polyvinylidenedifluoride (PVDF) membranes (Pall Life Science, Ann Arbor, MI). The membranes were blocked for 1 hr with 5% nonfat dry milk in TBS/T (10mM Tris-Cl, pH 7.6, 100mM NaCl and 0.1% Tween 20). The membranes were incubated with anti-nArgBP2 (1:1000), β-tubulin (1:1000), and anti-GFP (1:5000) primary antibodies for 2 hr at room temperature or overnight at 4°C, and then with HRP-conjugated secondary antibody for 1hr. The immunoreactions were detected with Supersignal West Pico chemiluminescent substrate (Thermo Scientific). After chemiluminescence detection using an ImageQuant LAS 4000 (GE Healthcare, Uppsala, Sweden), images were analyzed by the ImageJ software.

III. Results

RNA interference-mediated knock-down of nArgBP2 had a strong effect on dendritic spine development

To investigate the endogenous function of nArgBP2, RNA interference-mediated knock-down experiment was performed with a plasmid encoding nArgBP2-silence sequence. For a preliminary test, we used shRNA designed to contain six different target sequences recommended from Sigma and Dharmacon Co. We verified them to have knock-down effect. To maximize the efficiency and specificity of shRNA effect, single target sequence was selected and tested by expressing in HEK293T cells. Among six candidates, the shRNA#1 and #2 were highly working well (Data not shown). Previous pilot study implied that nArgBP2 knock-down in neurons had a strong inhibitory effect on synapse formation but enhanced the number of filopodia. Consequently, when nArgBP2 was barely expressed in cultured rat hippocampal neurons, we could observe low density of the dendritic spines and the increased number of filopodia in secondary dendrite branches representatively (Fig. 1A). Reduction of nArgBP2 expression was confirmed by westernblotting in HEK293T cells transfected with GFP-nArgBP2 (Fig. 1B). Quantification data showed that number of dendritic spines in control group ($n = 28.89 \pm 1.27$) was approximately three times as many as that of dendritic spines in the absence of nArgBP2 ($n = 7.97 \pm 1.10$). While there was few number of filopodia in normal developing neurons ($n = 0.64 \pm 0.19$) (14

to 16 DIV), relatively large number of filopodia was counted (n = 11.15 ± 0.90) (Fig. 1C). For objective classification of protrusions, terms were defined as follows. Filopodia implied to all thin headless protrusions on dendritic shafts and dendritic spines indicated mainly mushroom, and stubby-type protrusions on dendritic shafts. The rest of protrusions were categorized as irregular protrusions. Composition of each type of protrusions informed that the irregular protrusions were more shown in the knock-down group (Fig. 1D).

The morphological difference was directly caused by reduced expression of nArgBP2 in dendritic spines

Due to notable morphology change, we had to examine direct effects of nArgBP2 knock-down on the dendritic spines, and might exclude false positives. Rescue experiments were performed with RNAi-resistant nArgBP2 mutant. The rescue construct of nArgBP2 was made by using site directed mutagenesis with two-nucleotide substitution. Both shRNA#1 and RNAi-resistant nArgBP2 were co-transfected into rat hippocampal neurons. After more than three days, dendritic spines were rescued much the same as those of control group in the developing stage. GFP-tagged RNAi-resistant nArgBP2 was expressed more in dendritic spines than in dendrites, which implied that nArgBP2 was predominantly located in postsynaptic side (Fig. 2A). Quantification data showed that the number of dendritic spines in the rescue group (n = 31.08 ± 2.02) was indistinguishable from that of control spines (n = 28.89 ± 1.27) ($p>0.05$) (Fig. 2B). In addition, the expression level of GFP-

tagged RNAi-resistant nArgBP2 transfected in HEK293T cells was similar to that of normally expressed GFP-nArgBP2 and proved by immnunoblotting. To eliminate the possible artifacts from shRNA expression vector itself (pU6-mRFP was used in this study.), RNAi-scrambled one was also tested and confirmed by immunoblotting (Fig. 2C).

nArgBP2 was involved in dendritic spine formation, not maintenance

Until now, distinct effect of RNA-mediated interference of nArgBP2 expression has been observed in the developing neurons (14 to 16 DIV). To explore the time-dependent study, we checked the expression pattern of nArgBP2 in cultured cortical neurons from 2 to 20 days *in vitro*. Consistent with earlier reports, the band size was detected near 200 kDa in cortical neurons as well as astrocytes (Data not shown). As shown in figure 3A, the expression pattern of nArgBP2 can be characterized as increment in time-dependent manner. nArgBP2 was hardly detected in the early stage (2 to 6 DIV), but a comparably large amount of nArgBP2 was expressed in the developing (10 to 14 DIV) and mature stage (18 to 20 DIV). We then concluded expression profile of nArgBP2 in rat cortical neurons during embryonic development.

Accordingly, we tested RNA-mediated interference of nArgBP2 in the mature stage. While the morphological changes in the knock-down group were shown in the developing neurons, both control and knock-down groups

in the mature neurons displayed the very identical phenotype. The length of spine neck was shortening and the shape of dendritic spines was similar to mushroom or stubby type as they became mature (Fig. 3B). Quantification analysis indicated that the number of dendritic spines was similar in both control (n = 43.45 ± 3.15) and knock-down groups (n = 36.67 ± 2.47) (Fig. 3C). Taken together, the specific action of nArgBP2 in the developing stage makes it possible to expect that this synaptic protein has a critical role in dendritic spine formation.

Although the strong effect of shRNA interference of nArgBP2 expression in neurons was revealed, we carried out one more experiments for consistent results. Independent shRNA#2 was constructed and a series of experiments was undergone with the same procedures done previously. In the early stage (2 DIV) and the mature stage (19 DIV) of hippocampal neuron, we would expect not to find any difference between control and knock-down groups (Fig. 4A, 4C). Likewise, the results of knock-down in the developing stage and rescue experiments were the same as before so that the function of nArgBP2 was firmly proved (Fig. 4D, 4E).

Depletion of nArgBP2 altered the morphology and motility of dendritic spines

Despite the function of endogenous nArgBP2 in neuronal cells was revealed briefly, static structural explanation was still seen as insufficient. Therefore, live cell imaging was performed. We transfected YFP-PM(plasma membrane)

and either a virgin vector or shRNA#1 into control or knock-down group (10 to 12 DIV), and monitored the change of dendritic spine morphology (14 to 16 DIV). Time-lapse images were acquired at 5 sec of intervals for 5 min. At first glance, dendritic spines were usually motile with a certain shape alteration. By subtracting latter images to former ones in chronological order, we obtained dark graphic areas which presented the motility of both control and knock-down groups (Fig. 5A). As revealed by dark graphics areas and quantitative measurement of spine motility, the increased motility of dendritic spines on absence of nArgBP2 was found (Fig. 5A, 5B). Moreover, the structure of dendritic spines in nArgBP2 knock-down group was atypical from that of normal physiological dendritic spines. To identify how shapes were changed, a shape factor was calculated by MetaMorph Imaging software (Universal Imaging Corporation, West Chester, PA). The principle of shape factor calculation is based on the ratio by vertical and horizontal line. If the shape factor is a value of 1, the head of dendritic spine is round-type, and if below 1, even close to zero, the head of dendritic spine is likely to be elongated or varied irregular. Within a few minutes, the value of shape factor was fluctuated from 0.5 to 1 in control group, whereas from 0.3 to 0.8 in nArgBP2 knock-down group (Fig. 5C; spine 1). Additionally there were a few dendritic spines plotted 0.8 or 0.4 of shape factor, but they had little movements (Fig. 5C; spine 2). This suggested that the absence of nArgBP2 could modify the architecture of dendritic spines.

By plotting the shape factor values against time, we obtained more information, such as the rate of morphological changes. If the shape factor is

more fluctuating, the dendritic spines have the higher rate of morphological changes. However, no difference in rate of morphological changes between control and knock-down group through shape factor analysis was found. These results could be easily acquired by subtracting from the latter value to former one, and then the distribution showed no significant distinctness (Data not shown). Therefore, we determined that removal of nArgBP2 did not have influence on the rate of morphological changes.

nArgBP2 would be involved in regulation of actin cytoskeleton

In the developing neurons, nArgBP2 seemingly worked for well-designed structural construction of dendritic spines. We knew that architecture of dendritic spines is fulfilled with actin cytoskeleton. In particular, F-actin (filamentous actin) is a major formation in dendritic spines and plays an important role in supporting spine structure. Previous studies suggested that nArgBP2 is an adaptor protein as regulating signaling complexes related to actin cytoskeleton. To verify this hypothetical relation between nArgBP2 and actin cytoskeleton, we conducted FRAP (fluorescence recovery after photobleaching) experiments on a single dendritic spine in the developing stage (15 to 16 DIV). GFP-actin was co-transfected with control virgin vector or shRNA#1 into rat hippocampal neurons at 10 to 12 days *in vitro*. To analyze the movement of GFP-actin, a circular ROI containing the dendritic spine was selected and photobleached with an Argon 488 laser (Fig. 6A). The

recovery of GFP-actin fluorescence was recorded at 5 sec of interval for 5 min in a time-course manner (Fig. 6B). The fluorescence intensity of GFP-actin was steadily maintained before bleaching, and fluorescence disappeared effectively after bleaching for 7 sec. Subsequently, fluorescence intensity was slowly recovered (up to about 60 or 80 %) over 80 sec in both groups, illustrating a fraction of mobile actin (Fig. 6C). The rest of the mobile fraction would be an immobile fraction of actin (Materials and Methods). Followed by these parameters, it was revealed that mobile fraction of actin was increased in the depletion of nArgBP2 (Fig. 6D). This might be attributable to the results that nArgBP2 regulates F-actin stabilization on synaptic architecture. Collectively, regulation of nArgBP2 resulted in F-actin dynamics was investigated.

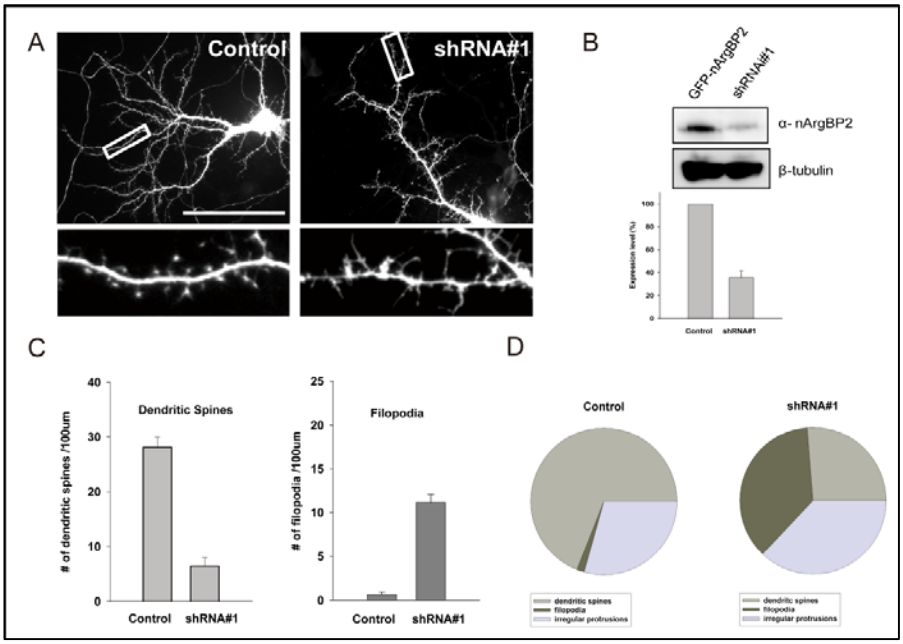

Figure 1. Knock-down of nArgBP2 in neurons showed a significant inhibition on dendritic spines formation and enhanced filopodia formation. (A) Representative images of hippocampal neurons in control and knock-down groups (15 DIV). In magnifying images, small and almost round shape of dendritic spines was dominantly presented (left), whereas long, and thin headless protrusions were easily found (right). (B) Immunoblotting results through HEK293T cells showing significant knock-down effects of shRNA#1 by expression of exogenous nArgBP2 with intensity quantification. (C) Quantitative data by counting the number of dendritic spines and filopodia, indicating less dendritic spine formation and more filopodia formation in absence of nArgBP2 function. (D) Two pi graphs illustrating the different portion of protrusion types with group categorization. These data were from 20 neurons each group. Scale bar: 100μm.

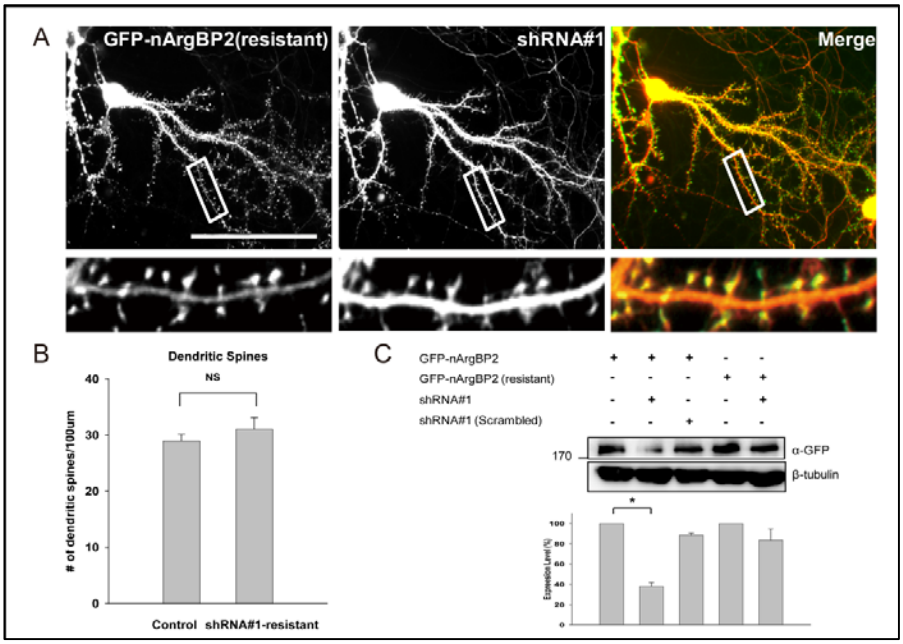

Figure 2. The shRNA#1-resistant produced dendritic spines similar to those of control group. (A) Representative images to show how well dendritic spines were recovered in numbers and phenotypes by GFP-tagged nArgBP2-resistant toward normal condition. (B) No significant differences were found in number of dendritic spines between control and shRNA#1-resistant groups (11 neurons, $p>0.05$). (C) Immunoblotting results displayed that GFP-nArgBP2-resistant form was expressed the same as GFP-nArgBP2 and strongly blocked shRNA#1 effects, and shRNA#1-scrambled one made little artifacts. Scale bar: 100μm.

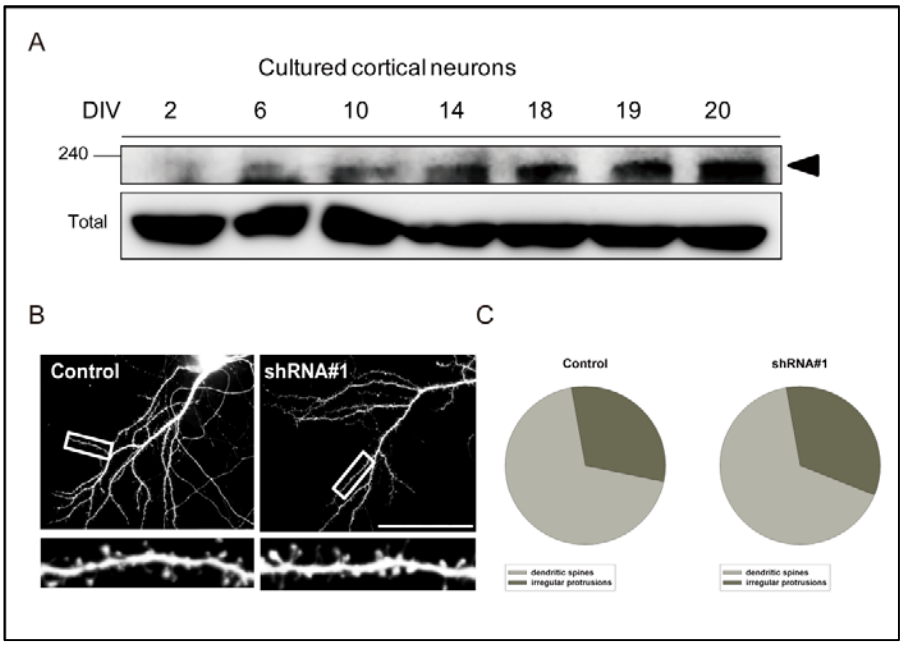

Figure 3. Expression pattern of nArgBP2 and representative images displayed no changes in number of dendritic spines in mature stage. (A) Increasing pattern of nArgBP2 expression from cultured cortical neurons (2 to 20 DIV). nArgBP2 was detected near 200 kDa. Total amounts of protein were 20μg, and detected by anti-nArgBP2 and anti-β-tubulin. (B) Representative images of hippocampal neurons in control and knock-down groups (19 DIV). In magnifying images, mushroom or stubby shape of dendritic spines was dominantly presented (left and right). (C) Two pi graphs showing similar portion of protrusion types with group categorization. 14 and 11 neurons were assayed each group. Scale bar: 100μm.

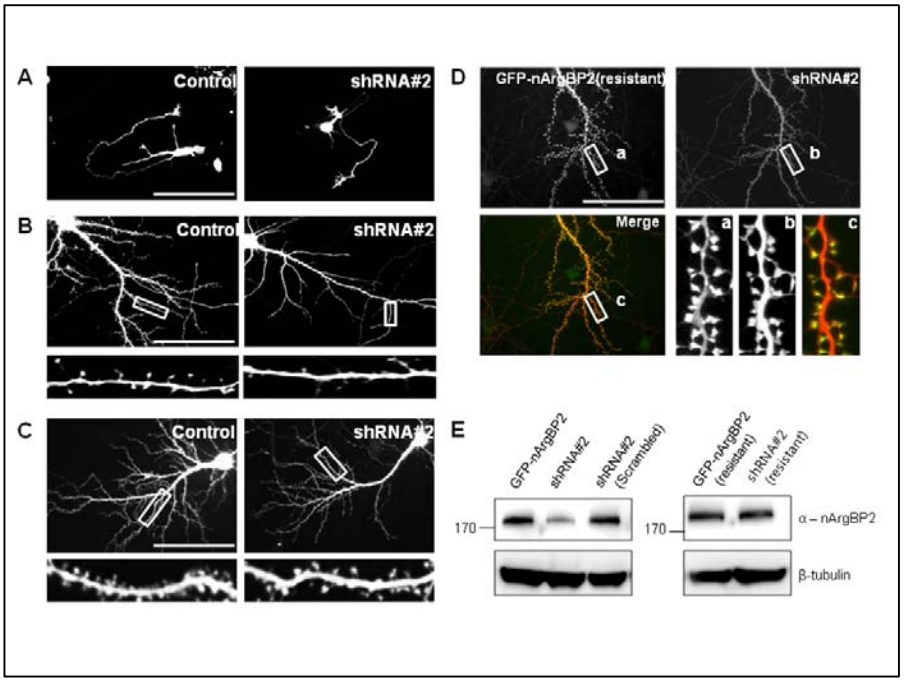

Figure 4. Another RNA interference-mediated knock-down of nArgBP2 firmly verified the same phenotype during dendritic spine development. The cell morphology in control and shRNA#2 groups during embryonic development at 2 DIV (A), 15 DIV (B), and 19 DIV (C). (D) The rescue experiments were successfully performed at 15 DIV. (E) Immunoblotting results displayed that shRNA#2 was effective without any artifact (shRNA#2-scrambled) and GFP-nArgBP2 resistant form was expressed the same as GFP-nArgBP2 and strongly prevented shRNA#2 effects. Scale bar: 100μm.

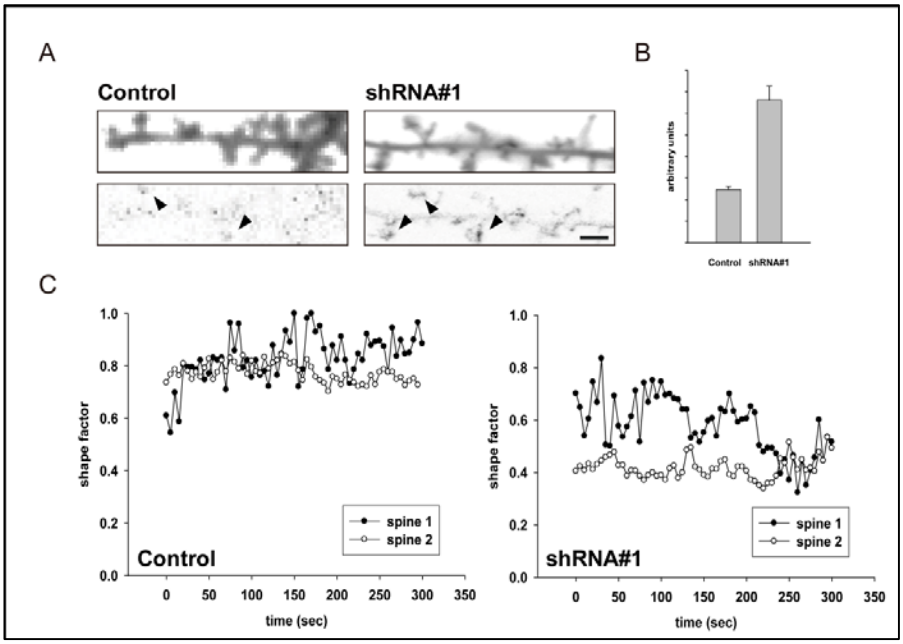

Figure 5. Increased motility in absence of nArgBP2 and different shapes in dendritic spines between control and knock-down groups were found during a time-lapse imaging. (A) Representative dendrite branch images in control and knock-down groups of nArgBP2 (upper) and gray graphics showed more dark areas indicating increased motility in knock-down group. Scale bar: 5μm. (B) Quantification of motility obtained from three small square ROIs of single dendritic spine. (C) Either motile or immotile dendritic spines were observed. Throughout shape factor analysis, value of 0.5 to 1 was presented in control group but value of 0.3 to 0.8 was measured in knock-down group. Totally 15 spines were randomly selected within a circular ROI, and analyzed for each group (see more details in texts).

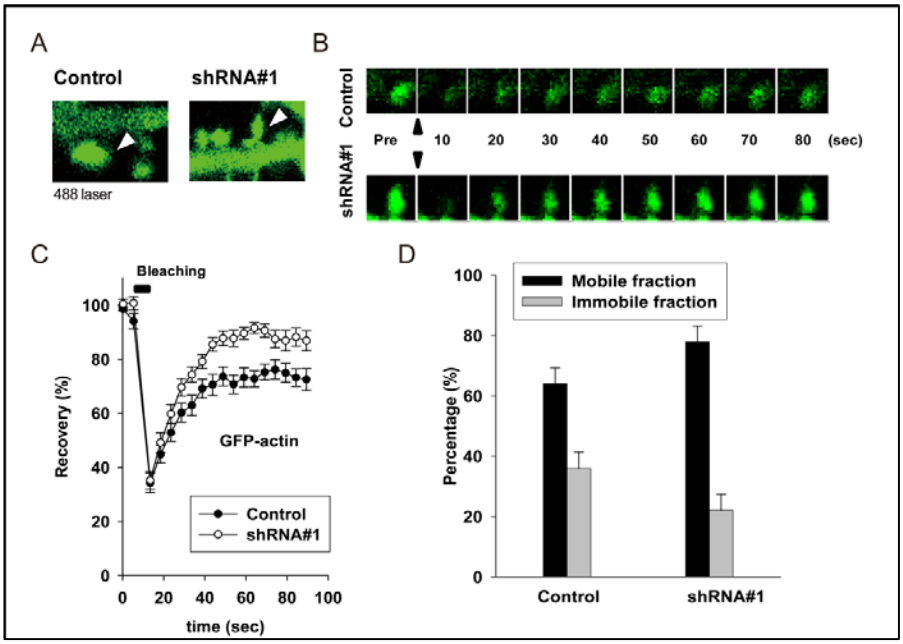

Figure 6. Actin dynamics in dendritic spines. (A) White indicators pointed target dendritic spines for FRAP experiments from confocal microscope images. (B) Sequential images from prebleaching to 80 sec (C) Fluorescence of GFP-actin was photobleached and recovered in control and knock-down groups within 80 sec. (D) Vertical bar graphs indicated shRNA#1 group had more mobile fraction than control group.

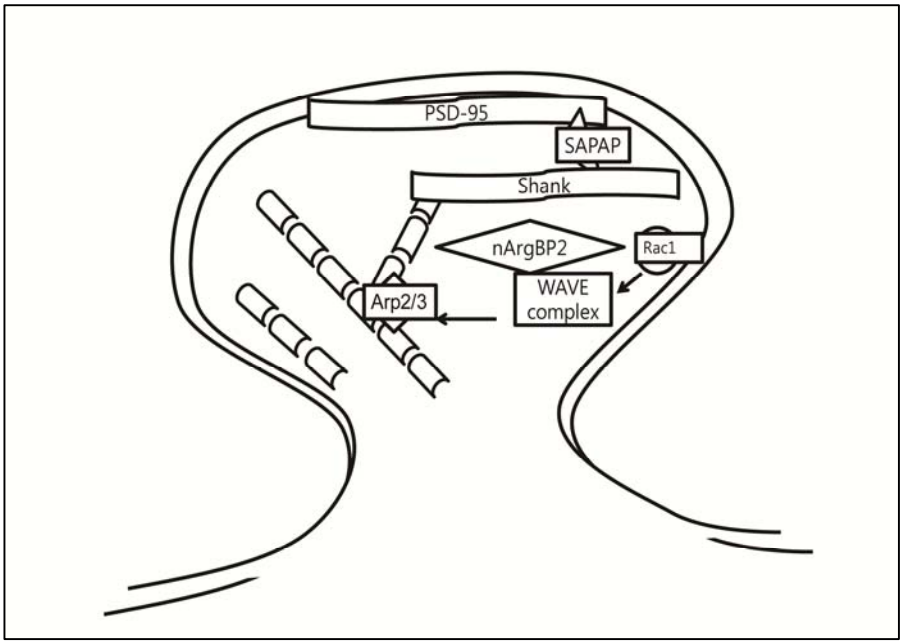

Figure 7. Hypothetical model. A hundreds of proteins took part in synaptic activity, consisting of networks in a small dendritic spine. Noted proteins were related to nArgBP2. These proteins were simplified for brief explanations. nArgBP2 directly interacted with WAVE complex, which received upstream signal of Rac1. Then WAVE complex induced Arp2/3 complex activated. During synaptic morphogenesis, the Arp2/3 complex made it possible to create protrusions in branch mode mainly by F-actin.

IV. Discussion

Here we revealed that the endogenous function of nArgBP2 at the synapses, in relation to structural changes with actin cytoskeleton. First of all, loss of nArgBP2 in the developing neurons could cause an evident morphological change toward reduction of dendritic spine density and filopodia formation. It was a direct effect of RNA interference-mediated knock-down of nArgBP2 proved by the rescue experiment. One would expect that overexpression of nArgBP2 could strengthen dendritic spine formation, but GFP-nArgBP2 expression in hippocampal neurons resulted in cell death. This was because high level expression of nArgBP2 disrupted the actin cytoskeleton and produced aggregates (22).

In order to expand the time-range of nArgBP2 working, investigating how dendritic spine morphology was altered in the early and mature stage was next direction for nArgBP2 study. Expression pattern of nArgBP2 in cultured cortical neurons was firstly testified that it showed an increase from 2 to 20 days *in vitro*. Based on this result, we compared the morphological changes in control and knock-down groups of the early stage, which could be remarkably monitored outgrowth of axons and dendrites, and guidance of the motile growth cone. But no significant dissimilarity between control and knock-down groups was observed because less nArgBP2 expressed in the early stage. In the same manner, phenotypic and quantitative analysis informed that the dendritic spines were well-formed with similar density in the mature stage. It

would support our data concerned about dendritic spine formation because effectiveness of shRNA mediated knock-down was validated only in the developing neurons. In addition, pilot experiments indicated that a strong reduction of synapses and mislocalization of PSD95 and synaptobrevin in 24 DIV knock-down neurons were observed. (Unpublished data, G. Cestra & Pietro) This might cast some clues with the fact that nArgBP2 strongly binds to SAPAP (synapse-associated protein 90 postsynaptic density-95-associated protein), which links PSD-95 and shank (25) (Fig. 7). Therefore, nArgBP2 took effects on not only dendritic spine formation but also presumably synaptic functions.

When it comes to the shape of dendritic spines, we showed here that more irregular structures were found in nArgBP2 knock-down group. Mostly dendritic spines were round type in normal physiological condition, whereas thin or wide, irregular types were shown in knock-down group from live cell time-lapse imaging. In motility test, the results showed that nArgBP2 had a critical function to maintain regular structure of dendritic spines. When nArgBP2 was absent in postsynaptic side, irregular-shaped dendritic spines were abundant and they had quite high motility. In astrocytes, nArgBP2 knock-down exhibited membrane ruffles so that it was seen as maintaining the balance between adhesion and motile behaviors (22). From the shape factor measurement, the rate of morphological change of dendritic spines could be calculated considering degree of fluctuation. However, there was no statistically significance in degree of fluctuation. Throughout image analysis, we focused on an external shape, not intrinsic molecular mechanisms.

Therefore, FRAP experiment was carried out. By adding GFP-actin into hippocampal neurons, we could discover relationship between nArgBP2 and actin cytoskeleton. It suggested that nArgBP2 functions to stabilize F-actin movements. In the absence of nArgBP2, F-actin was turned out to be more mobile. Since nArgBP2 did not directly connect to F-actin, it was still difficult to explain only with those results.

Hypothetically, we suggested the explanations in relation to nArgBP2 binding partners, WAVE isoforms. In a previous report, anchored WRP associated with WAVE 1 showed morphological changes in the ratio of spine head/filopodia in hippocampal slices as likely as we described here (8). Likewise, nArgBP2 combined with WAVE1,2, implying that activating WAVE regulatory complex by phosphorylation and inducing Arp2/3 complex to branch at 70° from original filamentous actin for stabilization of dendritic spines. This hypothetical statement could explain why irregular shape of dendritic spines was more prevalent in the absence of nArgBP2 (Fig. 7).

Furthermore, this study might not be limited to mammalian animals, but rather be applied for human disease study. The target sequence of shRNA#1 for nArgBP2 knock-down was all commonly present in rats, mice, and human isoforms. We could expect the similar phenotypes. Moreover, nArgBP2 knock-out mice suggested that disruption of nArgBP2 gene might cause psychiatric disorder such as bipolar disorder verified from behavior tests. (Guoping Feng Lab; US Patents. Pub. No.:US 20100077493 A1)

In short, we established the function of nArgBP2, one of genetic controls of synaptic morphogenesis by using RNA-mediated interference for

knock-down study and an image analysis for observation of morphological changes. An intracellular mechanism for nArgBP2 was thought to be closely related to actin regulation and its binding partners, WAVE and SAPAP.

V. References

1. Matus A. Growth of dendritic spines: a continuing story. Current opinion in neurobiology. 2005;15(1):67-72.

2. Sheng HHaM. Dendritic spines : structure dynamics and regulation. NATURE REVIEWS Neuroscience. 2001.

3. Bhatt DH, Zhang S, Gan WB. Dendritic spine dynamics. Annual review of physiology. 2009;71:261-82.

4. Vicente-Manzanares M. Dendritic spine similarities with protrusions and adhesions in migrating cells. The Open Neuroscience Journal. 2009.

5. Hotulainen P, Hoogenraad CC. Actin in dendritic spines: connecting dynamics to function. The Journal of cell biology. 2010;189(4):619-29.

6. Hering H, Sheng M. Activity-dependent redistribution and essential role of cortactin in dendritic spine morphogenesis. The Journal of neuroscience. 2003;23(37):11759-69.

7. Wegner AM, Nebhan CA, Hu L, Majumdar D, Meier KM, Weaver AM, et al. N-wasp and the arp2/3 complex are critical regulators of actin in the development of dendritic spines and synapses. Journal of Biological Chemistry. 2008;283(23):15912-20.

8. Soderling SH, Guire ES, Kaech S, White J, Zhang F, Schutz K, et al. A WAVE-1 and WRP Signaling Complex Regulates Spine Density, Synaptic Plasticity, and Memory. Journal of Neuroscience. 2007;27(2):355-65.

9. Takenawa T, Suetsugu S. The WASP-WAVE protein network:

connecting the membrane to the cytoskeleton. Nature reviews Molecular cell biology. 2007 Jan;8(1):37-48. PubMed PMID: 17183359.

10. Innocenti M, Zucconi A, Disanza A, Frittoli E, Areces LB, Steffen A, et al. Abi1 is essential for the formation and activation of a WAVE2 signalling complex. Nature cell biology. 2004;6(4):319-27.

11. Gautreau A, Hsin-yi HH, Li J, Steen H, Gygi SP, Kirschner MW. Purification and architecture of the ubiquitous Wave complex. Proceedings of the National Academy of Sciences of the United States of America. 2004;101(13):4379-83.

12. Suetsugu S, Kurisu S, Oikawa T, Yamazaki D, Oda A, Takenawa T. Optimization of WAVE2 complex–induced actin polymerization by membrane-bound IRSp53, PIP3, and Rac. The Journal of cell biology. 2006;173(4):571-85.

13. Kurisu S, Takenawa T. WASP and WAVE family proteins: Friends or foes in cancer invasion? Cancer science. 2010;101(10):2093-104.

14. Ismail AM, Padrick SB, Chen B, Umetani J, Rosen MK. The WAVE regulatory complex is inhibited. Nature structural & molecular biology. 2009 May;16(5):561-3. PubMed PMID: 19363480. Pubmed Central PMCID: 2716658.

15. Lebensohn AM, Kirschner MW. Activation of the WAVE Complex by Coincident Signals Controls Actin Assembly. Molecular Cell. 2009;36(3):512-24.

16. Pocha SM, Cory GO. WAVE2 is regulated by multiple phosphorylation events within its VCA domain. Cell motility and the cytoskeleton. 2009 Jan;66(1):36-47. PubMed PMID: 19012317. Pubmed

Central PMCID: 2798068.

17. Takenawa T, Miki H. WASP and WAVE family proteins: key molecules for rapid rearrangement of cortical actin filaments and cell movement. Journal of cell science. 2001;114(10):1801-9.

18. Choi J, Ko J, Racz B, Burette A, Lee JR, Kim S, et al. Regulation of dendritic spine morphogenesis by insulin receptor substrate 53, a downstream effector of Rac1 and Cdc42 small GTPases. The Journal of neuroscience. 2005;25(4):869-79.

19. Mitsushima M, Sezaki T, Akahane R, Ueda K, Suetsugu S, Takenawa T, et al. Protein kinase A-dependent increase in WAVE2 expression induced by the focal adhesion protein vinexin. Genes to cells : devoted to molecular & cellular mechanisms. 2006 Mar;11(3):281-92. PubMed PMID: 16483316.

20. Kawabe H, Hata Y, Takeuchi M, Ide N, Mizoguchi A, Takai Y. nArgBP2, a novel neural member of ponsin/ArgBP2/vinexin family that interacts with synapse-associated protein 90/postsynaptic density-95-associated protein (SAPAP). Journal of Biological Chemistry. 1999;274(43):30914-8.

21. Strakowski SM, Delbello MP, Adler CM. The functional neuroanatomy of bipolar disorder: a review of neuroimaging findings. Mol Psychiatry. 2005 Jan;10(1):105-16. PubMed PMID: 15340357.

22. Cestra G, Toomre D, Chang S, De Camilli P. The Abl/Arg substrate ArgBP2/nArgBP2 coordinates the function of multiple regulatory mechanisms converging on the actin cytoskeleton. Proceedings of the National Academy of Sciences of the United States of America. 2005 Feb 1;102(5):1731-6. PubMed PMID: 15659545. Pubmed Central PMCID: 547834.

23. Chang S, De Camilli P. Glutamate regulates actin-based motility in axonal filopodia. Nature neuroscience. 2001;4(8):787-93.

24. Bae J, Sung BH, Cho IH, Song WK. F-Actin-Dependent Regulation of NESH Dynamics in Rat Hippocampal Neurons. PloS one. 2012;7(4):e34514.

25. Yao I, Iida J, Nishimura W, Hata Y. Synaptic localization of SAPAP1, a synaptic membrane-associated protein. Genes to Cells. 2003;8(2):121-9.

Abbreviation

ABI	Abelson-interacting protein
Abp1	Actin-binding protein 1
Arp2/3	Actin-related protein 2/3
Cdc42	cell division cycle 42
CYFIP1	cytoplasmic FMR1-interacting protein 2
DIV	Days *in vitro*
FRAP	Fluorescence recovery after photobleaching
HEK293T	Human Embryonic Kidney 293 T
HSPC300	Haematopoietic stem/progenitor cell protein 300
HRP	Horse Radish Peroxydase
IRSp53	Insulin Receptor Substrate p53
mDia	mouse Diaphanous
NAP1	Nick-associated protein-1
N-WASP	neural Wiskott-Aldrich syndrome protein
PIP_2	phosphatidylinositol (4,5)-bisphosphate
PIP_3	phosphatidylinositol (3,4,5)-triphosphate
PIR121	Homo sapiens p53 inducible protein
PKA	Protein Kinase A
PSD-95	Postsynaptic density 95
ROI	Region of interest
SAPAP	synapse-associated protein 90/postsynaptic density-95-associated protein

shRNA	small hairpin RNA
VCA region	verprolin homology domain, cofilin homology domain, acidic region
WAVE	WASP-family verprolin homology protein
WRP	WAVE-associated RacGAP protein

요약 (국문 초록)

수상돌기 가시(dendritic spine)는 작지만 많은 액틴으로 구성된 돌출부로서 시냅스가소성에 중요한 역할을 하는 흥분성 시냅스 전달을 받아들여 작동한다. 하나의 수상돌기 가시는 수백여 개의 시냅스 조절 단백질로 구성되어 있다. 무수하게 많은 결합단백질이 시냅스 조절과 관련한 기능을 설명하고 있음에도 불구하고, nArgBP2에 대한 우리의 이해는 단지 비신경세포에서 확인된 사실로부터 추론하는 수준에 그치고 있다. nArgBP2는 ArgBP2의 신경세포특이적으로 mRNA 수준에서 편집된 결합단백질로서 시냅스 후 부위에 풍부하게 존재한다. Ponsin/ArgBP2/Vinexin family의 한 구성요소로서 N 말단 부위에 sorbin homology (SoHo) 도메인, 가운데에는 zinc finger, C 말단 부위에는 세 개의 src homology 3 (SH3) 도메인을 갖고 있다. SH3 도메인을 통해서 nArgBP2는 SAPAP, dynamin, synaptojanin, WAVE 이형체들과 결합 짝으로서 상호작용 한다.

RNA 간섭을 통해 nArgBP2 기능이 상실되면 수상돌기 가시 발달에 강한 변화가 나타난다. 발달단계에서 nArgBP2 기능이 상실되면 수상돌기 가시의 수가 감소하는 반면, 수상돌기 돌출부(filopodia)는 더 만들어진다. RNA 간섭 저항 돌연변이를 사용하여 회복실험을 수행했다. shRNA#1과 RNA 간섭 저항 돌연변이를 함

께 주입하고 난 뒤, 발달 단계에서 대조군과 같은 수준으로 수상돌기 가시가 생겼다. nArgBP2는 시냅스 형성을 유도하는 데 관여하지만 유지하는 데는 관련성이 떨어진다. nArgBP2가 발현하는 패턴을 날짜 별로 보면 증가한다. 19~20일에 nArgBP2 기능상실을 유도한 결과 수상돌기 가시의 수에서 변화가 보이지 않았다. 실시간 세포영상을 통해 nArgBP2 기능상실로 인해 발달단계의 배양 해마 신경세포의 수상돌기 가시의 형태와 운동성이 변화한다는 사실을 밝혔다. 광표백후 형광복구 실험을 통해 nArgBP2 기능상실 실험군에서 증가된 액틴 운동성을 조절한다는 사실은 시냅스 구조에서 nArgBP2가 액틴을 조절한다는 것을 알려준다. 결론적으로 이는 nArgBP2가 액틴을 조절함으로써 시냅스 형태형성에서 중요한 기능을 담당함을 의미한다.

주요어: 수상돌기 가시, 수상돌기 돌출부, RNA 간섭, 액틴 동역학, 웨이브(WAVE), 시냅스 형태형성

학 번: 2010-20399